scientific reports

Check for updates

OPEN

Omacetaxine reduces c-Myc expression and demonstrates antitumor effects in osteosarcoma

Kristen B. Farrell✉, Sunetra Das & Douglas H. Thamm

Omacetaxine mepesuccinate (OMX), formerly known as homoharringtonine, is a protein translation inhibitor approved for use in human chronic myeloid leukemia. Recent studies suggest that OMX may be effective against other cancer types, and may be successful against protein targets that are otherwise difficult to inhibit by reducing their translation rates. Using canine, human, and mouse osteosarcoma (OS) cell lines, we investigated the antineoplastic effects of OMX against OS by evaluating growth inhibition, migration and invasion, apoptosis, expression of c-Myc, changes in gene expression, and *in vivo* efficacy. OMX induced dose-dependent growth inhibition and apoptosis of OS cells with IC_{50} values in the low nanomolar range. OMX also reduced migration and Matrigel invasion. Strikingly, levels of c-Myc protein were reduced in most canine, human, and mouse OS cell lines after OMX exposure, and Myc target RNA transcripts were also reduced with treatment. OMX significantly inhibited tumor growth in and metastasis in two separate orthotopic mouse OS models. OMX is a promising candidate for treatment of OS in both dogs and humans, and potentially other c-Myc-driven cancers.

Keywords Osteosarcoma, Omacetaxine, c-Myc, Canine cancer, Protein translation

Abbreviations

DEG	Differentially expressed gene
GSEA	Gene set enrichment analysis
OMX	Omacetaxine
OS	Osteosarcoma

Osteosarcoma (OS) is the most common primary bone tumor in both humans and dogs. Treatments for OS have not advanced in three decades, resulting in a stagnation of survival expectations for both species[1,2]. Although OS is rare in humans with about 1,000 new cases per year in the United States, it is more common in canine patients, especially large breed dogs, with about 10–20,000 cases per year[3,4]. OS is pathologically indistinguishable between human and canine cases, and the disease progresses similarly in both species, although with a compressed timeline in dogs. The spontaneous development of the disease, similar pathology, an accelerated disease progression associated with the comparatively shorter canine lifespan, and increased case numbers, all make canine OS an attractive model for OS research[5–10].

Omacetaxine mepesuccinate (OMX), also known as homoharringtonine, or brand name Synribo™ (Teva Pharmaceuticals), is an FDA approved treatment for human chronic myeloid leukemia with tyrosine kinase inhibitor resistance[11,12]. OMX is a protein translation inhibitor that functions by blocking the A site of the ribosome to prevent amino acid chain elongation[13]. Although clinical studies using OMX are limited to hematological malignancies[12,14], some preclinical research has shown promising function in other tumor types. Multiple studies demonstrate the effects of OMX on various cell signaling pathways and induction of apoptosis in several solid tumor types[14].

c-Myc is a transcription factor regulating multiple essential processes such as cell division and apoptosis, and is constitutively or over-expressed in the majority of cancers, including OS[15]. c-Myc is difficult to directly inhibit due to its largely disordered structure lacking binding pockets for small molecule inhibitors, along with principally nuclear localization of the protein[16]. However, reduction of c-Myc levels has been observed after OMX treatment in hematological malignancies[17,18], a phenomenon that has also been demonstrated using other methods of translational inhibition[19,20]. C-Myc has a short cellular half-life of approximately 25 min[21,22]; thus, blocking translation of new c-Myc results in degradation via proteolysis without replacing the protein

Flint Animal Cancer Center, Department of Clinical Sciences, Colorado State University, 1620 Campus Delivery, Fort Collins, CO 80523, USA. ✉email: Kristen.farrell@colostate.edu

with nascent amino acid chains. OMX was also shown to indirectly reduce c-Myc by binding NKRF (NF-κB repressing factor), preventing p65 from binding the c-Myc promoter[18].

To assess the potential use of OMX against OS, we evaluated the anticancer properties of OMX in human, canine, and mouse OS cell lines by measuring growth inhibition, apoptosis, migration, and invasion. Orthotopic mouse models were then used to evaluate efficacy of OMX against OS *in vivo.* Additionally, we examined c-Myc protein levels in OS cells after OMX treatment and also observed associated transcriptional changes.

Materials and methods

Cell culture and growth inhibition assays

Canine tumor-derived cell lines[23] were authenticated by species-specific PCR and STR analysis as described previously[24], and all cell lines were tested for mycoplasma prior to use. Cultures were maintained at 37 °C in a humidified atmosphere of 5% CO_2 and passaged using trypsinization (Corning). All cells were cultured using Dulbecco's Modified Eagle Medium (DMEM) supplemented with 10% fetal bovine serum, MEM vitamin solution, 2 mM L-glutamine, 1 mM sodium pyruvate, non-essential amino acids, and antibiotic/antimycotic solution (Corning). Drug sensitivity assays were conducted as described previously[25]. Briefly, cells were seeded overnight before media was replaced with media containing OMX (Homoharringtonine, Millipore Sigma) or corresponding DMSO control of equal concentration, with additional agents included for combination studies. After a 72-hour incubation in treated media, resazurin (200 µg/mL in PBS, MP Biomedicals) was added and fluorescence was measured with a Bio-Tek Synergy HT Multi-Mode Microplate Reader (Agilent). Five technical replicates were used per condition, and the experiment was performed independently three times for each cell line. Results were combined into a total of 15 replicates per data point. Relative viable cell number was expressed relative to the DMSO control matched to the highest drug concentration. For non-attachment assays, 96-well plates were coated with poly-HEMA ((Poly 2-hydroxyethyl methacrylate) Millipore Sigma) by applying a 20 mg/mL solution in ethanol to each well and drying overnight at 37 °C before storing at room temperature until use in drug sensitivity assays.

Reagents

Omacetaxine (Homoharringtonine, Millipore Sigma) was prepared to a 10 mM solution in DMSO, aliquoted and stored at −80 °C until use. VDC-597 (VetDC Inc) was prepared to a 10 mM solution in DMSO, aliquoted and stored at −80 °C until use. Bortezomib (Millipore Sigma) was prepared to a 10 mM solution in DMSO, aliquoted and stored at −80 °C until use. Doxorubicin was obtained from the CSU Veterinary Teaching Hospital Pharmacy in a sterile preparation of 2 mg/ml and stored at −20 °C until use.

Protein synthesis assay

Nascent protein synthesis was measured using Protein Synthesis Assay Kit (Cayman Chemical) as per manufacturer's instructions. This kit introduces O-propargyl-puromycin to cells and terminates translation upon incorporation into the C terminus of elongating polypeptide chains, then uses click chemistry to attach a fluorescent molecule to the polypeptide chain. Cells were treated with 50 nM OMX, cycloheximide, or DMSO control for 4 h. Fluorescence was measured using a Beckman Coulter Gallios flow cytometer and analyzed using FlowJo (BD) software.

Live cell imaging

Live cell imaging was performed as described previously[25]. Briefly, cell lines expressing Nuclight Red™ (Essen Bioscience) were seeded into 96-well plates overnight. Media was then replaced with media containing omacetaxine or an equivalent DMSO control, along with cell death indicator YOYO™−1 Iodide (491/509) (Invitrogen) at 100 nM. Images were acquired every 6 h following treatment using an IncuCyte Zoom live cell imaging system (Sartorius), and images were analyzed using IncuCyte Zoom software. Four images per well were averaged, and five replicate wells per condition used to generate each data point with $n = 5$.

Cell cycle analysis

Cell cycle analysis was performed as previously described[25]. Briefly, cells were treated with10 nM omacetaxine or equivalent volume of DMSO for 24 h before fixing and resuspending in 500 µL FXCycle PI/RNase Staining Solution (Molecular Probes) for 15 min. Cells were then assessed using a Beckman Coulter Gallios flow cytometer and analyzed using FlowJo (BD) software.

Migration and invasion assays

Migration assays were performed as previously described[25]. Briefly, cells were serum-starved overnight before plating with drug treatment in the top chamber of Boyden chambers (8.0 µm pores) (Corning) in a 24-well plate, or Matrigel coated Boyden chambers (8.0. µm pores) (Corning) for invasion analysis. Complete media filled the lower well outside of the chamber and cells were allowed to incubate in chambers for 18 h. Non-migrated cells were then removed from the top of the membrane before staining with Diff-Quik for brightfield imaging. Each treatment was repeated across two membranes. Cell numbers from five 10x magnification fields of each membrane (10 total per condition) were quantified using ImageJ (NIH), and percent growth inhibition measured in a simultaneous resazurin assay was accounted for in the final totals.

Western blot

Western blots were performed as described[25]. Briefly, cells were plated in 6-well plates overnight before incubating with specified drug concentrations for 4 h unless otherwise indicated. Cells were then rinsed with PBS and lysed with lysis buffer in the plate. Lysates were measured for protein content using a BCA Assay (Biorad) and

loaded for SDS-PAGE in equal total protein concentrations. Primary antibodies anti-c-Myc (Abcam, ab32072 Rb mAb to c-Myc) and anti-cofilin (Cell signaling, Cofilin D3F9 XP Rabbit mAb) were used at 1:1000 dilution and incubated at 4 °C overnight. Secondary antibody was used at a 1:40,000 dilution and incubated for 1.5 h at RT (Goat anti-rabbit IgG HRP-conjugated ,Thermo Scientific).

RNA extraction and sequencing

Cells were plated overnight in 6-well plate at 50% confluency. The following day, media was replaced with media containing 50 nM OMXor DMSO control. After 6 h, cells were washed with PBS, then lysed in plate using the RNeasy (Qiagen) RLT buffer with 2-mercaptoethanol. The lysate was then applied to QIAshredder (Qiagen) before completing the RNeasy protocol with DNase digestion as per manufacturer's recommendations. Purified poly-A RNA was stored at −80 C until further processing. RNA purity, quantity and integrity were determined by NanoDrop (ThermoFisher Scientific) and TapeStation 4200 (Agilent) analysis prior to RNA-seq library preparation.

The mRNA-seq libraries were generated from 200 ng of total RNA using the *Universal Plus™ mRNA-Seq with NuQuant®* kit (Tecan Genomics) following the manufacturer's instructions. Briefly, RNA underwent poly(A) selection, fragmentation, cDNA synthesis, end repair, adapter ligation with Unique Dual Indexes (UDIs), and PCR amplification, yielding Illumina-ready libraries. Libraries were sequenced on a NovaSeq X Plus platform (Illumina), generating 150 bp paired-end reads at a target depth of ~40 million per sample. Sequencing was performed at the Genomics Shared Resource, University of Colorado Anschutz Medical Campus (RRID: SCR_021984). Base calling and demultiplexing of raw sequencing data were carried out with *bcl2fastq* (Illumina) using default parameters.

RNAseq data processing

Paired-end RNA-seq reads from dog and mouse samples (59–77 million reads per sample) were aligned to the CanFam3.1 (Ensembl v104) and GRCm39 (Ensembl v114) reference genomes, respectively, using STAR (v2.7.10b) alignment tool[26]. Gene-level counts were obtained with *featureCounts* (subread v2.1.1)[27]. Differential expression analysis between control DMSO-treated ($n = 3$) and OMX-treated ($n = 3$) cell lines was performed using *DESeq2*[28]. Briefly, genes with fewer than five counts in at least two samples were filtered out. Following filtering, counts were normalized using size factors, and differential expression was assessed with the DESeq function. Differentially expressed genes (DEGs) were defined as those with an absolute log2 fold change > 2 and an adjusted p-value < 0.05.

Differentially expressed genes (DEGs) were subjected to pathway enrichment analysis using gene set enrichment analysis (GSEA) implemented in the *clusterProfiler* R package[29]. GSEA was performed on a ranked gene list, ordered by log2 fold change and associated significance, against the Molecular Signatures Database (MSigDB) collections (https://www.gsea-msigdb.org/gsea/msigdb), including Hallmark, Reactome, BioCarta, PID, KEGG Legacy, and Oncogenic signature gene sets[30]. Analyses were carried out with 10,000 permutations, using gene sets with a minimum size of 10 and a maximum size of 200 genes. Enriched pathways were considered significant at a false discovery rate (FDR)–adjusted p-value < 0.05.

Transcription factor activity analysis

High-confidence (confidence levels A and B) transcriptional regulons specific to *Mus musculus* were obtained from the DoRothEA database[31]. These regulons define curated transcription factor (TF)–target relationships annotated with the *mode of regulation* (MOR), indicating whether a TF is known to activate (+1) or repress (−1) a given target gene. Using only high confidence transcriptional regulons, we analyzed targets for 123 transcription factors.

To infer transcription factor (TF) activity, we applied the Univariate Linear Model (ULM) approach implemented in the decoupleR R package. This method estimates TF activity scores by modeling the expression of each TF's downstream target genes—weighted by their MOR sign—against the observed log-transformed, normalized gene expression (logCPM). The resulting activity scores reflect the collective regulatory impact of each TF on its targets across each sample, accounting for both activating and repressive interactions.

Mouse studies

All mouse studies were performed in an AALAC-approved facility at Colorado State University with the approval of the Institutional Animal Care and Use Committee (IACUC protocol #3590). All methods were conducted in compliance with applicable guidelines and regulations. Female athymic nude mice (Jackson Laboratories) and female C3H mice (Jackson Laboratories) were aged 6–8 weeks upon arrival and were allowed to acclimate for at least 7 days prior to study initialization. Mice had an average weight of 22.1 ± 1.0 g (nude) and 21.9 ± 1.4 g (C3H) at study initialization, and all mice had continuous access to food and water ad libitum. Mice were euthanized upon losing 15% body weight, when largest tumor diameter exceeded 10 mm, or when significant lameness or a decline in body condition score was observed. Tumor volume was calculated as an ellipsoid from caliper measurements at the largest length and width dimensions of the hindlimb distal segment. The ellipsoid volume of the contralateral unaffected leg was subtracted to estimate the tumor volume. A tumor diameter requiring euthanasia measured 10 mm above the normal leg diameter on the contralateral unaffected limb. Euthanasia was performed by CO_2 inhalation until complete cessation of breathing for a minimum of 2 min, followed by cervical dislocation.

Orthotopic osteosarcoma mouse models

Tumors were established using intratibial injections of 500,000 cells in a 50% Matrigel (Corning) solution by drilling a 25G needle into the top of the tibia in mice anesthetized with inhaled 3% isoflurane as described

in Farrell et al.[32]. Four days after injection, tumor establishment was confirmed using luminescence imaging described below, and randomized into treatment groups. Homoharringtonine (Millipore Sigma) was dissolved in sterile PBS with heat and sonication for use in the mouse injections, and drug preparation was tested using growth inhibition assays in vitro to confirm potency equal to DMSO preparation used in in vitro experiments. Treated mice received 1 mg/kg injected intraperitoneally five days weekly for the duration of the studies, while equal volume of sterile PBS was used as a mock treatment. Mice were weighed and tumor diameters measured at least twice weekly.

In vivo imaging

Tumors were imaged in live mice as described previously[32] using an IVIS Spectrum system with Living Image software (version 4.5.1, Perkin Elmer). Briefly, Luciferin (Potassium salt, GoldBio) was injected subcutaneously into each mouse 10 min prior to imaging. Images were collected with up to five mice simultaneously, while separated by luminescence-blocking barriers in lateral recumbency with the tumor-bearing leg facing up, followed by imaging in sternal recumbency for thorax acquisition. Tumor luminescence intensities were measured using Living Image software with equally sized regions of interest over the entire luminescent region and quantifying the total flux (photons/sec).

Statistical analysis

Statistical analyses were conducted using GraphPad Prism 9 (GraphPad Software), and include student's t-test, one-way ANOVA, two-way ANOVA, and log-rank (Mantel Cox). Drug combination synergy analysis was performed using Synergy Finder 3[33]. Error bars denote standard deviation (SD) unless otherwise indicated. P values less than 0.05 are indicated with a single asterisk (*), less than 0.01 with two asterisks (**), less than 0.001 with three asterisks (***), and less than 0.0001 with four asterisks (****).

Results

Omacetaxine inhibits growth and translation in OS

Sensitivity to OMX of OS cell lines from three species was tested *in vitro.* Cells were grown in the presence of various OMX concentrations for 72 h before measuring resazurin fluorescence indicative of live cells. The average IC_{50} values in seven canine OS cell lines ranged from 1.6 nM to 19.9 nM, six human OS cell lines ranged from 4.5 nM to 56.7 nM, and two mouse OS cell lines from 10.7 nM to 114 nM (Fig. 1A-C). These values are near or below the 46 nM single and 66 nM multi-dose human plasma C_{Max} for OMX delivered subcutaneously[34], suggesting that concentrations capable of reducing OS cell growth are achievable in human patients. Growth inhibition curves were similar in cells grown with or without attachment (Figure S1A), suggesting that circulating OS may also be sensitive to OMX. Combination treatment with the common clinical OS therapy doxorubicin indicated an additive relationship (Figure S1B). Next, we assessed the ability of OMX to reduce protein translation in three cell lines to confirm the mechanism of action across species. OMX significantly reduced protein translation similar to the positive control cycloheximide in human, canine, and mouse OS cell lines (Fig. 1D).

Next, live cell imaging was used to confirm growth inhibition and assess cell death. OS cells expressing NucLight Red were grown in the presence of various OMX concentrations as well as YOYO-1 iodide for 72–96 h with Incucyte imaging every 6 h. Red cell counts (cells/FOV) showed reduced growth rates with increasing concentrations of OMX across human, canine, and mouse OS cell lines (Fig. 2A-C). Dead cells, indicated by green fluorescence from YOYO-1 iodide DNA intercalation, also increased with OMX concentration (Fig. 2D). No significant changes in cell cycle distribution were observed after 24 h of OMX treatment (Figure S1C), suggesting that cell death is the main contributor to growth inhibition.

Omacetaxine treatment reduces migration and invasion capability of OS cells

The effects of OMX on migration and invasion capabilities of OS cells were then measured using Boyden chamber assays. Cells were serum starved overnight before plating on top of a membrane containing 8 µm pores along with 0, 10, or 50 nM OMX. Media containing 10% FBS was supplied in the lower chamber as a chemoattractant, and cells migrating through the membrane were quantified. To measure invasion, the membrane was coated in Matrigel requiring degradation by cells before accessing the porous membrane. Growth inhibition was also measured in separate wells during the same time frame to account for any reduction in cell number in the treated cell totals. The number of human, canine, and mouse OS cells able to migrate to the outside of the membrane was significantly reduced with increasing OMX concentration (Fig. 3A-D), and invasion through Matrigel was similarly reduced (Figure S2A-B).

Omacetaxine reduces c-Myc protein levels

Next, protein levels of c-Myc were measured in OMX treated cells. c-Myc has a short half-life and undergoes rapid proteasomal degradation[21,22], suggesting that a block in protein translation of new amino acid chains would result in rapid reduction in expression. Western blots of OS cell lines treated with 50 nM OMX for 4 h indicate a reduction in c-Myc protein levels in the majority of cell lines across species (Fig. 4A). Basal expression of c-Myc measured by RNAseq in untreated canine cell lines did not correlate with OMX IC_{50}, nor with amount of of c-Myc protein via western blot, nor amplification[35](Figure S3A-B, Table 1). The cell lines contain various known mutational drivers[8,36,37], which also have no obvious correlation with sensitivity (Table 1). The observed reduction in c-Myc protein level was dependent on dose of OMX (Fig. 4B, S4A), and also time and drug-washout dependent (Fig. 4C, S4B). Our collection of canine OS cells exhibit c-Myc expression via RNAseq comparable to our other canine cell line cancer types (Figure S5A), suggesting that other cancer types may also exhibit c-Myc reduction and sensitivity to OMX treatment.

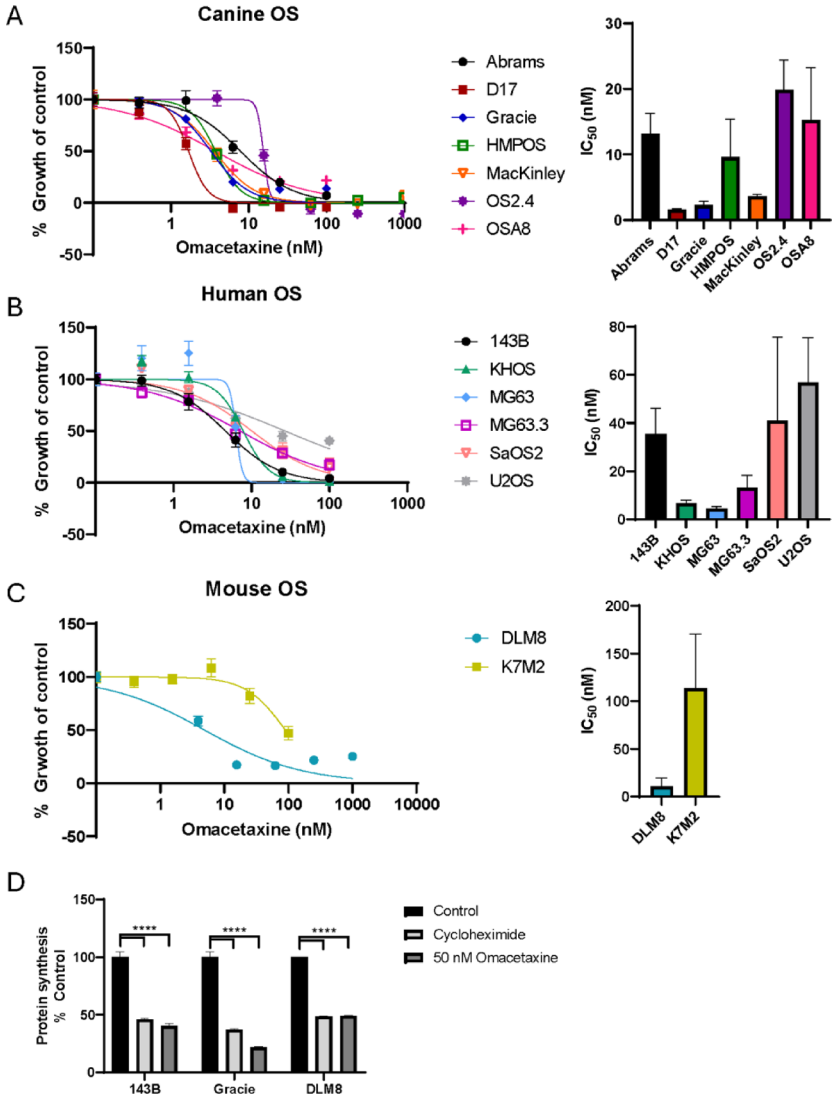

Fig. 1. Omacetaxine inhibits growth and translation in OS. **(A)** Canine OS cell lines were grown in various concentrations of OMX for 72 h before measuring resazurin fluorescence. Each cell line was repeated at least three times, and IC_{50} values of each separate experiment were averaged. **(B)** Human OS cells. **(C)** Mouse OS cells. Error bars represent SD. **(D)** Protein synthesis was measured using OPP incorporation into elongating polypeptide chains in untreated cells, or cells treated with OMX or positive control cycloheximide for 4 h. Error bars represent SD. **** $p < 0.0001$.

Omacetaxine reduces tumor growth in orthotopic mouse models

OMX was then assessed for efficacy against OS in vivo using an orthotopic model of OS via intratibial injection of cells. Starting four days following injection, mice were treated 5x weekly with intraperitoneal injections of 1 mg/ml OMX or saline and measured for tumor volume and bioluminescence. The canine OS cell line Gracie showed a significant reduction in OS growth by caliper measurement (Fig. 5A-B) and luminescence quantification of tibia and thorax (Fig. 5D-E). OMX treated mice also had significantly increased survival before qualification for euthanasia (Fig. 5C). Mice did not lose weight throughout the experiment and had no observable effects from treatment (Fig. 5F).

We then evaluated OMX efficacy in a syngeneic orthotopic mouse model. DLM8 cells were implanted into immune competent C3H mice via intratibial injection and treated as in the immune compromised model. Tumor volume was significantly reduced in the OMX-treated mice by caliper measurements (Fig. 5G-H), as well as bioluminescence measured in the thorax (Fig. 5J). The increase in survival time and primary tumor growth measured via bioluminescence were not statistically significant (Fig. 5I-J), although some individual mice showed very little primary tumor growth with treatment (Fig. 5H). Again, OMX-treated mice did not lose weight throughout the experiment (Fig. 5L), nor exhibit any signs of health deficit during treatment. C-Myc levels in canine OS tumor tissue collected from treated mice trended towards reduced c-Myc expression via western blot but the decrease was not statistically significant (Figure S6).

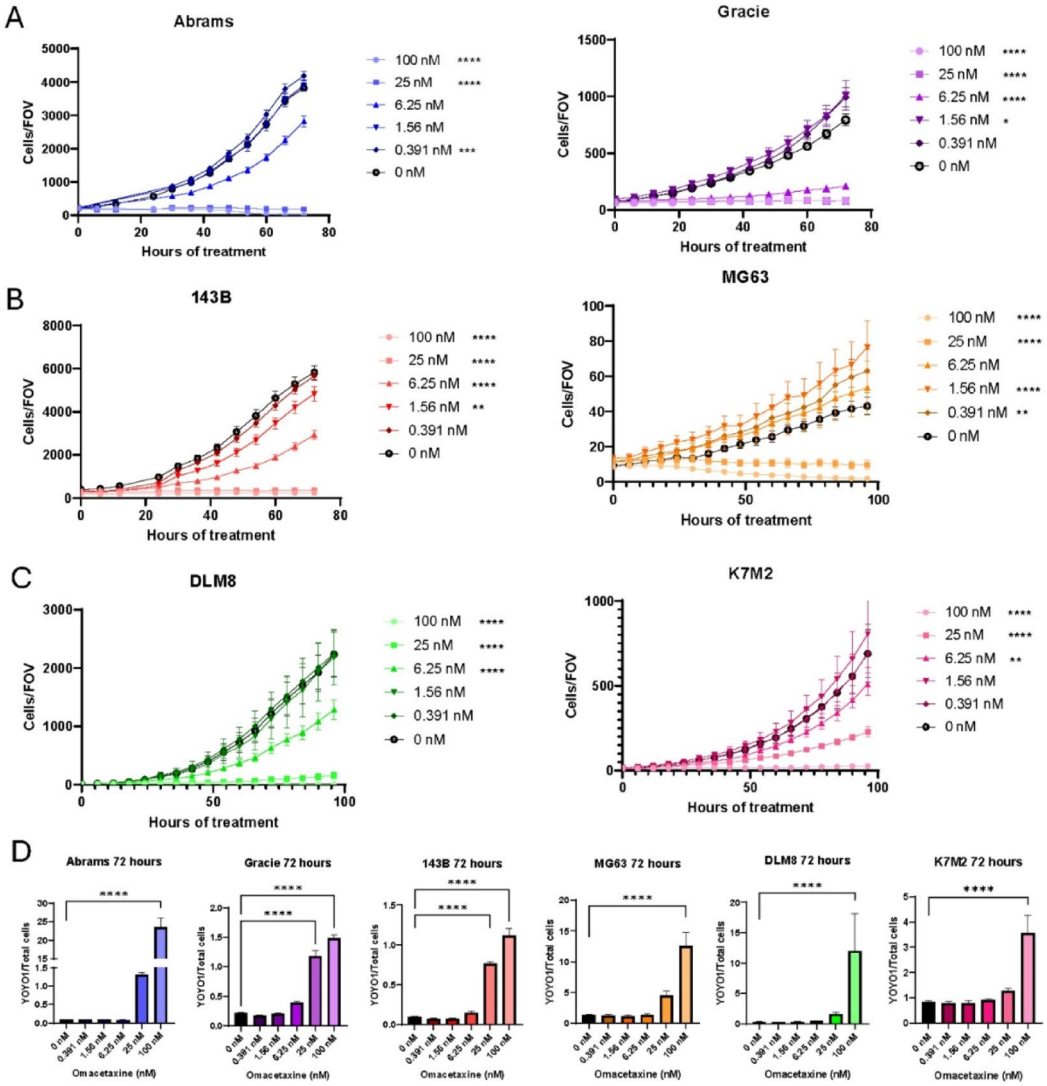

Fig. 2. Live cell imaging demonstrates growth inhibition and cell death induction in OMX treated OS cells. **(A)** Canine OS cells labeled with Nuclight Red fluorescence were grown in the presence of various OMX concentrations and 100 nM YOYO-1 iodide with imaging every 6 h. The number of red fluorescent cells per imaged field of view are averaged across 4 images per well, then five replicate wells. Asterisks indicate statistical difference from control treatment. **(B)** Human OS cells. **(C)** Mouse OS cells. **(D)** The average number of red fluorescent cells in each well was divided by the number of green fluorescent cells (representing apoptotic cells) to demonstrate a live to dead cell ratio. Error bars represent SD. Statistical significance was assessed using a two-way ANOVA with multiple comparisons comparing column means (A-C) or one-way ANOVA with Tukey's multiple comparison test (D). **** $p < 0.0001$, *** $p < 0.001$, ** $p < 0.01$, * $p < 0.05$.

Omacetaxine reduces transcription of c-Myc target genes

We then selected the cell lines demonstrating efficacy in mouse models for further analysis via RNAseq. Gracie and DLM8 cells were treated with OMX in vitro for 6 h before RNA isolation and sequencing. DLM8 cells had 644 differentially expressed genes (DEGs) with OMX treatment, Gracie cells had 458, and 63 of the DEGs were in common between the two cell lines (Fig. 6A-C, Figure S7A-B, Table S1-2,5). One of the top DEGs in both cell lines was *GADD45B*, a growth arrest and DNA damage response gene that is transcriptionally downregulated by c-Myc[38,39]. Other genes known to be downregulated in response to an increase in Myc showed a consistent increase with OMX treatment (Figure S8). The degree of overlap may be underestimated as comparing the different species may omit genes with varying or without direct orthologs; thus, we assessed the pathways represented by the significant DEGs. GSEA pathway analysis of the DEGs showed DLM8 cells with 193 significantly changed pathways and Gracie cells with 80, with an overlap of 57 pathways in common between the species. Notably, both cell lines showed a significant decrease in expression of Myc target genes (Fig. 6D-F, Table S3-4,6), supporting our finding of reduced c-Myc protein levels. Significant changes in individual genes represented in the GSEA human gene set of Hallmark Myc Targets V1 are present in both species (Fig. 6G-H), and Hallmark Myc Targets V2 was additionally significant in the mouse cells (Figure S8C). To confirm continuity of c-Myc target gene lists

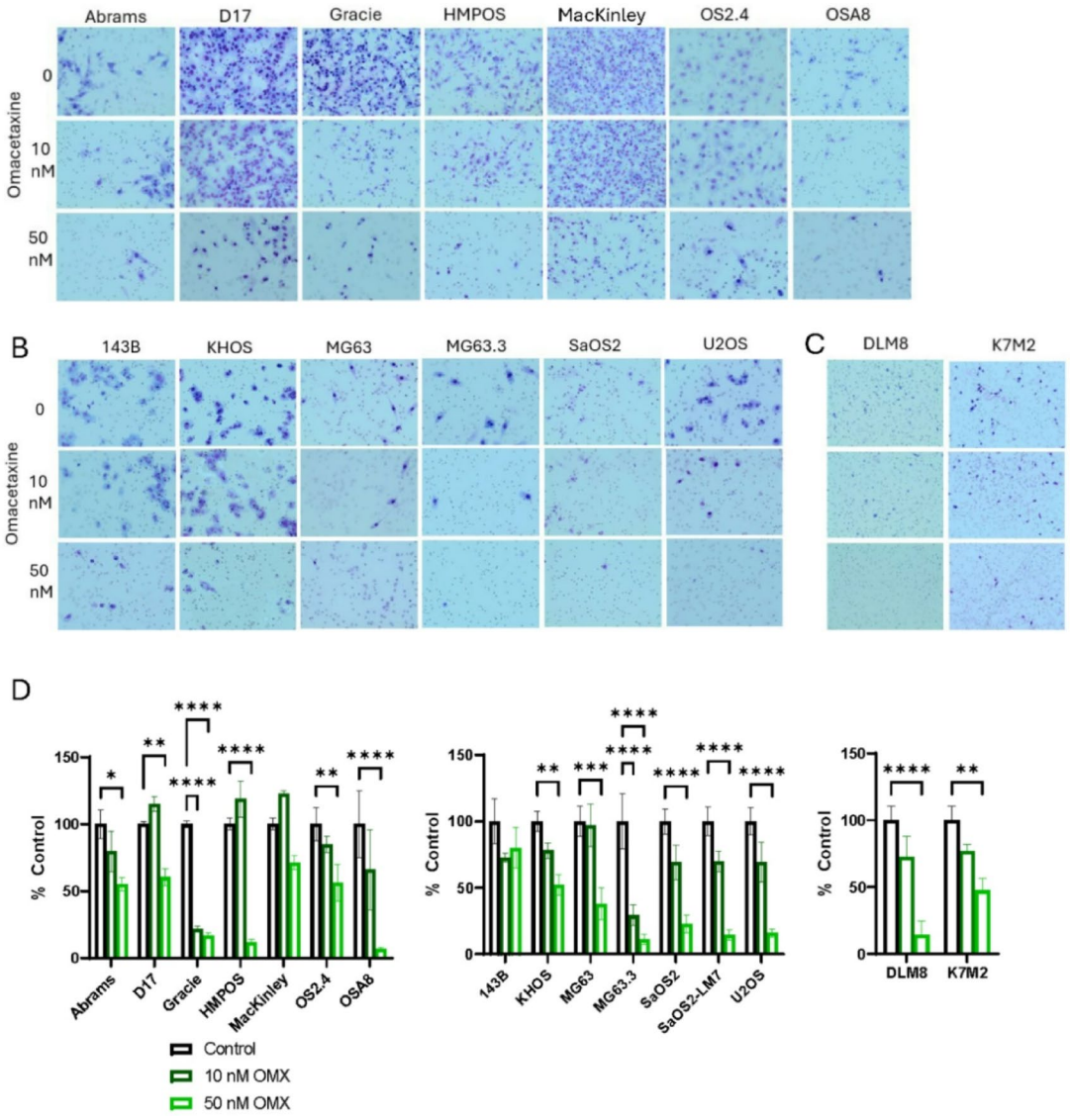

Fig. 3. Omacetaxine treatment reduces migration capability of OS cells. **(A)** Representative images of stained canine OS cells migrated across a porous membrane with 10 nM or 50 nM OMX treatment or DMSO control. **(B)** Human OS cells. **(C)** Mouse OS cells. **(D)** Quantification of 10 fields imaged for each treatment condition, normalized to control treated cells. Error bars represent SD. Statistical significance was assessed using a two-way ANOVA with multiple comparisons. **** $p < 0.0001$, *** $p < 0.001$, ** $p < 0.01$, * $p < 0.05$.

developed from human studies on canine cells, we confirmed that steady state RNAseq data from untreated canine OS cells demonstrated an increase in up-regulated Myc target genes, and decrease of down-regulated Myc target genes, demonstrating consistent patterns in canine cells. This does not change across canine OS cell lines at moderately higher or lower Myc expression levels (Figure S5B).

Other pathways that were significant in both cell types include upregulation of TNFα signaling via NFκB, and downregulation of mTORC1 signaling. To interrogate the potential therapeutic relevance of these two pathways, we treated Gracie and DLM8 cells with a combination of OMX and bortezomib, a proteosome inhibitor which acts as an NFκB inhibitor[40–42], or VDC-597, a combination PI3K and mTOR inhibitor[43,44]. These two combinations showed synergy at some concentrations in these OS cell lines and warrant further investigation for combination treatments (Figure S9).

We further assessed changes in transcription factor activity using Discriminant Regulon Expression Analysis (DoRothEA)[31]. This analysis was limited to the mouse cell line DLM8, as regulon data is not experimentally confirmed in the canine genome. The activity of multiple transcription factors was significantly affected by OMX treatment, with either increased or decreased activity (Fig. 6I, S10). Notably, this analysis further confirmed our finding of decreased Myc activity with OMX treatment, and reveals additional potential targets of interest in cancer cell growth and immunology.

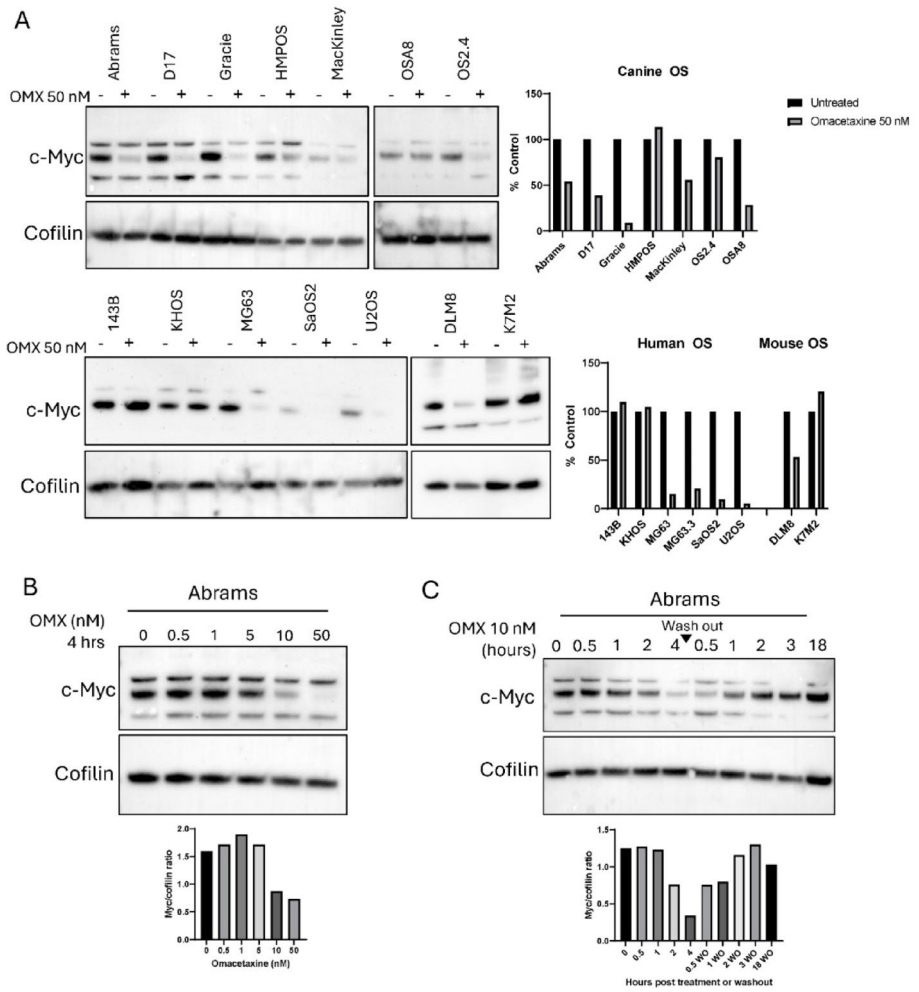

Fig. 4. Protein levels of c-Myc are reduced with OMX treatment. **(A)** Canine, human, and mouse OS cells were treated with 50 nM OMX or DMSO control for 4 h before cell lysates were collected and assessed for c-Myc expression via western blot. Quantification was adjusted to cofilin loading control before normalizing to control treatment. **(B)** Abrams cells were treated with varying concentrations of OMX for 4 h before cell lysates were collected and assessed for c-Myc expression via western blot. Quantification was adjusted to cofilin loading control before normalizing to control treatment. **(C)** Abrams cells were treated with 10 nM OMX for varying times before cell lysates were collected. After 4 h, cells were washed 2x with PBS before returning to untreated media for specified times when lysates were collected. Quantification was adjusted to cofilin loading control before normalizing to control treatment. Original uncropped blots are presented in supplementary data.

Cell line	Gene	Mutation type	HGVS.*p*	MYC amplification	c-Myc RNAseq Log2 Transcripts per Million (TPM)	Species
Abrams	TP53	Missense	C267F	No	12.2	Canine
D17	KRAS	Missense	E63K	Borderline gain	12.5	Canine
Gracie	SRGAP3	Frameshift	V850fs	No	12.5	Canine
HMPOS	MET, TP53	Missense	R1188Q, R164H	Yes	13.1	Canine
MacKinley	PPM1D, MED12	Stop-gained, Frameshift	E472Ter, L1938fs	No	11.2	Canine
OS2.4	TP53	Missense	I222T	Borderline gain	11.6	Canine
OSA8	KDM6A	Frameshift	T986fs	Borderline gain	12.1	Canine
SAOS2	SPEN	Missense	V1208G	Data Not available	Data Not available	Human
143B	TP53	Missense	R156P	Data Not available	Data Not available	Human
U2OS	PPM1D	Stop-gained	R458Ter	Data Not available	Data Not available	Human
MG63	ATRX	Missense	D412G	Data Not available	Data Not available	Human

Table 1. Mutational drivers and c-Myc amplification in human and canine osteosarcoma cell lines[8,36,37].

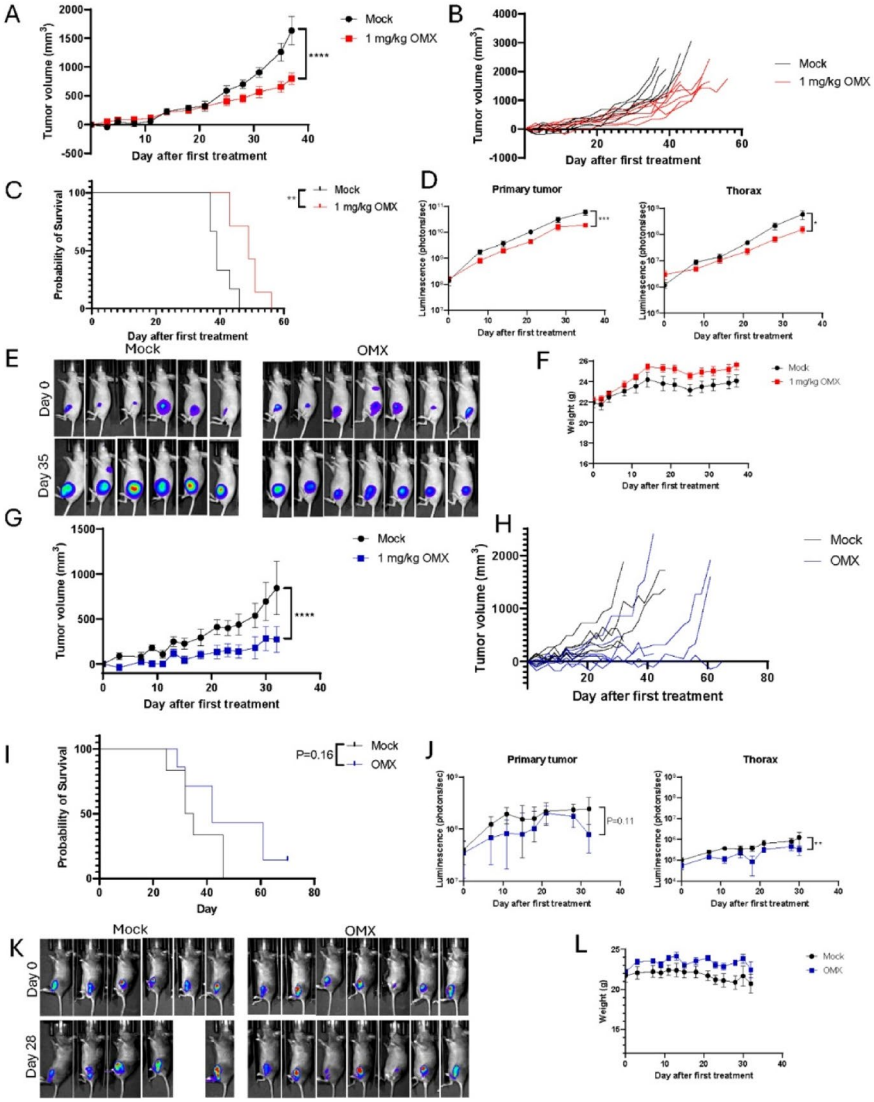

Fig. 5. Omacetaxine reduces OS tumor growth in orthotopic mouse models. **(A)** Gracie-LUC cells were injected intratibially into nude mice four days before randomization into groups treated with 1 mg/kg OMX or mock saline injection 5x weekly. Tumor volume was measured with calipers by subtracting volume of the non-inoculated limb from the tumor-bearing limb. **(B)** Spaghetti plot visualizing the tumor volume growth progression of each individual mouse. **(C)** Survival of mice until meeting criteria for euthanasia. **(D)** Quantified luminescence (photons/sec) measured in equal size ROIs over the inoculated tibia or thorax. **(E)** Images of luminescence on the first day of treatment (day 0) and after 35 days. **(F)** Weights of mice over the course of the experiment. **G-L)** DLM8-LUC cells were injected into syngeneic C3H mice and treated as above. Error bars represent SD. Statistical significance was assessed using a two-way ANOVA with multiple comparisons (A, D, G, J) or Log-rank (Mantel-Cox) test (C, I). **** $p < 0.0001$, *** $p < 0.001$, ** $p < 0.01$, * $p < 0.05$.

Discussion

Osteosarcoma patients face the same treatment options that were available decades ago, with little advancements in survival times or prognosis, especially for patients with metastasis. This study demonstrates the efficacy of a protein translation inhibitor against OS, opening the door for a new class of drug in the arsenal against OS. Human, canine, and mouse OS cells were sensitive to OMX at pharmacologically relevant concentrations[34], demonstrating growth inhibition, apoptosis, reduced migration and invasion capacities, and reduced tumor growth *in vivo* in orthotopic xenogeneic and syngeneic mouse models. Furthermore, OMX reduced the level of c-Myc protein in OS cells and significantly reduced transcription of c-Myc target genes.

Many additional transcriptional pathways were significantly altered after OMX treatment, opening opportunities for further studies identifying additional mechanisms of action for OMX, and potential therapeutic combinations. Other groups have already identified potential combination targets specific to other cancer types, such as immunomodulatory drugs combined with OMX in multiple myeloma[17], and reactive oxygen species

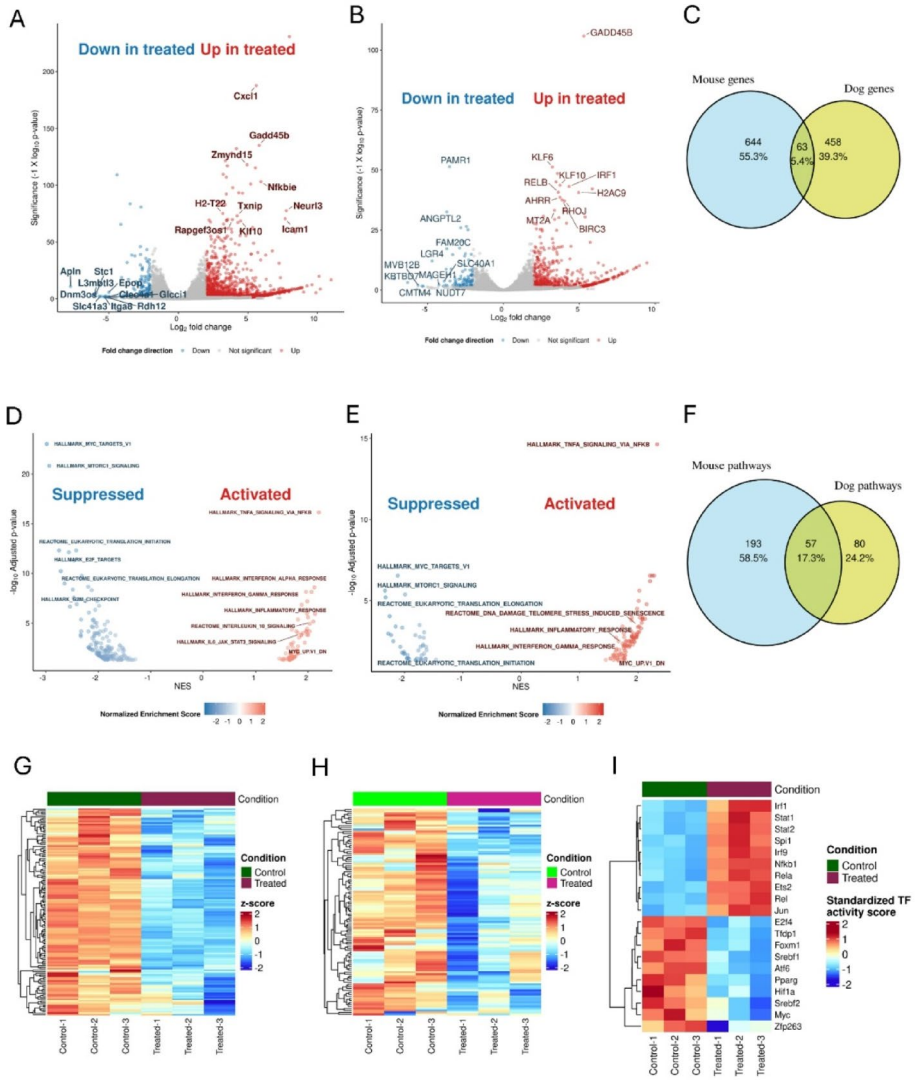

Fig. 6. Omacetaxine reduces transcription of c-Myc targets. **(A)** DLM8 cells (mouse) or **(B)** Gracie (dog) cells were treated with 50 nM OMX or DMSO control for 6 h before collecting RNA for sequencing. Significant differentially expressed genes are visualized in a volcano plot and full lists are available in supplemental materials (Table S1-2). **(C)** Venn diagram of mouse and canine DEGs, highlighting 5.4% common orthologous genes. **(D)** Enriched pathways identified from pre-ranked GSEA in DLM8 and **(E)** Gracie cell lines are represented as volcano plots. Selected pathways relevant to this study were noted on the plots. The full lists of enriched pathways are available in supplemental materials (Table S3-4). **(F)** Venn diagram of mouse and canine enriched pathways, highlighting 17.3% overlapping pathways. Core enriched genes from GSEA gene set "Hallmark Myc Targets V1" show decrease in transcripts following OMX treatment in both DLM8 **(G)** and Gracie **(H)** cells. **I)** Heatmap showing the top 10 upregulated and top 10 downregulated transcription factors (TFs) based on regulon activity scores from DLM8 RNA-seq data, identified using the *DoRothEA* database following OMX treatment.

were identified as an effective combination with rocaglate-based eIF4A inhibitor against OS[19,20], which acts similarly to a translation inhibitor through a slightly different target. Reactive oxygen species did not appear in our pathway analysis after OMX treatment, thus this slight difference in drug mechanism of action may be sufficient to change effective drug combinations. In hepatocellular carcinoma, protein levels of five oncoproteins including c-Myc were reduced with OMX treatment, and translation of multiple cell division-related genes were downregulated[45]. These downregulated genes include E2F1, which reinforces our finding of significant downregulation of E2F targets in both the canine and murine DEG pathway analysis (Table S3-4,6), as well as the mouse transcription factor activity (Fig. 6C, S10, Table S7).

The relevance of some pathways which show significance in the analysis can be complicated to interpret as many pathways have overlapping gene sets, such as "Reactome Eukaryotic Translation Initiation", which includes many eukaryotic translation initiation factors which are also Myc target transcripts. Regardless, we identified the NFκB pathway and mTORC1 signaling as potential future combination therapy targets due to significant

changes in transcription in both cell lines with OMX treatment. OMX in combination with an mTOR inhibitor was found to be effective against multiple myeloma cells, and cells with a developed resistance to OMX had a partial restoration of sensitivity to OMX with mTOR inhibition[46]. A combination of OMX and bortezomib in vitro displayed synergy against OS cell lines, expanding the potential reach of this combination which has previously shown efficacy against hematological malignancies[14,46-48]. We have now demonstrated potential efficacy of these combinations in a solid tumor type.

Though our interest in bortezomib originated as a known inhibitor of the NFκB pathway, a combination treatment targeting both protein synthesis and protein degradation provides an intriguing rationale for disrupting cellular metabolism at multiple points. Targeting two different cellular survival strategies may reduce the ability to adapt to metabolic changes or develop resistance. However, the effects on c-Myc degradation after OMX treatment in the presence of bortezomib have not been examined and may significantly affect the pathways identified in this study. Additionally, both bortezomib and OMX have significant side effects in patients, thus the combination would require attention to toxicities. Alternative proteosome inhibitors may offer a safer combination, such as FDA-approved Carfilzomib, which offers greater specificity for the proteosome and decreased peripheral neuropathy, or orally administered Ixazomib, which additionally offers an extended half-life[42].

The results garnered by the transcription factor activity analysis also open many possibilities for alternative uses and targets for OMX. Effects on immune function may be indicated by significant changes in transcription factors such as STAT1, STAT2, IRF1, IRF9, NFκB family, etc. However, transcript changes are difficult to decipher without further experimentation, as increased transcript levels may not result in changes in protein level due to the inhibition by OMX. Thus, detailed studies are required before further interpretation.

The OS cell lines demonstrated varying levels of c-Myc reduction after OMX treatment, but this did not correlate with IC_{50} value, suggesting either that small levels of c-Myc reduction are sufficient to reduce growth rate or induce cell death in some cell lines, or that inhibition of translation of other proteins are substantially contributing to antitumor effects. Nevertheless, all OS cell lines were sensitive to OMX treatment at low to moderate nanomolar concentrations, similar to serum levels measured in human patients[34]. As OMX has previously only been used clinically in human hematological malignancies, the ability of the drug to penetrate solid tumors may require additional investigation, as our xenograft models displayed non-significant decreases in c-Myc expression, though this may be due to bulk tumor tissue collection and cell type heterogeneity. Drug sensitivity data available on DepMap[36,37], reveal that bone neoplasms have one of the lowest average AUC values in response to OMX, behind lymphoid, myeloid, and peripheral nervous system cell types. This corroborates our finding of in vitro sensitivity, yet more in vivo studies are necessary to evaluate efficacy against solid tumors.

Although OMX pharmacokinetics have not been evaluated in canine patients, assessment of protein translation inhibition in canine cell lines suggests that the mechanism of action translates across species; thus, OMX could be an effective option for canine patients with OS. Canine patients offer a valuable opportunity to test OMX in spontaneously arising OS, with a compressed disease progression timeframe and higher number of patients available for clinical trials[3–5].

The action of OMX against OS cell lines expressing high levels of c-Myc, and the specific reduction of c-Myc protein levels and associated target transcripts, gives rise to the potential use of OMX against other cancer types dependent on c-Myc or high levels of protein translation. Metastatic cells depend on high levels of protein translation[49–51], thus OMX may show increased efficacy against metastatic cells. Our studies demonstrated growth inhibition of non-adhered OS cells, reduced migration and invasion capacities in treated cells, as well as significant reduction of luminescent cells in the lung in both of our orthotopic mouse models. Further studies are required to separate effects of OMX specifically against metastatic cells.

Despite FDA approval of OMX for human chronic myeloid leukemia and promising clinical work in acute myeloid leukemia[52], the manufacturer has recently discontinued production of the drug Synribo. OMX may have fallen out of favor due to side effects or the requirement of twice daily injections, despite the approval for patients to perform subcutaneous injections at home[12]. Severe side effects include thrombocytopenia, neutropenia, and anemia, among others[11,12,14]. Recent studies have investigated increasing bioavailability and new delivery methods which may reduce these side effects[14]. Non-pharmaceutical-grade experimental quantities of OMX remain available from multiple manufacturers, allowing continued study of OMX as a promising drug candidate for OS and other cancers.

Conclusions

Omacetaxine shows robust activity against osteosarcoma *in vitro* and *in vivo*. OMX treatment demonstrates downregulation of c-Myc and its target genes, revealing pan-cancer implications for this widely dysregulated pathway. This investigation of omacetaxine expands the application of this drug from its FDA approved indications to potential use in solid tumors such as osteosarcoma in both human and canine patients.

Data availability

All data generated by this study is provided in the supplementary materials or available in the GEO database with accession # GSE316004 (https://www.ncbi.nlm.nih.gov/geo/query/acc.cgi?acc=GSE316004).

Received: 22 January 2026; Accepted: 15 April 2026
Published online: 21 April 2026

References

1. Panez-Toro, I. et al. Advances in Osteosarcoma. *Current Osteoporosis Reports,* **21,** 330–343 (2023). https://doi.org/10.1007/s11914-023-00803-9
2. Sheng, G., Gao, Y., Yang, Y. & Wu, H. Osteosarcoma and metastasis. *Front. Oncol.* 11:780264. https://doi.org/10.3389/fonc.2021.780264 (2021).
3. Bone Cancer in Dogs. *American Kennel Club Canine Health Foundation* (2010). https://www.akcchf.org/disease-history/bone-cancer-in-dogs/
4. About Osteosarcoma. *American Cancer Society* (2020). https://www.cancer.org/content/dam/CRC/PDF/Public/8768.00.pdf
5. Gustafson, D. L., Duval, D. L., Regan, D. P. & Thamm, D. H. Canine sarcomas as a surrogate for the human disease. *Pharmacology and Therapeutics*. **188,** 80–96 (2018). https://doi.org/10.1016/j.pharmthera.2018.01.012
6. Klosowski, M. et al. Naturally occurring canine sarcomas: Bridging the gap from mouse models to human patients through cross-disciplinary research partnerships.. *Front. Oncol.* **13**:1130215. https://doi.org/10.3389/fonc.2023.1130215 (2023).
7. McGee, L.E., Pereira, J.S., McEachron, T.A. et al. The tumor microenvironment of metastatic osteosarcoma in the human and canine lung. *Commun Biol* **8**, 756 (2025). https://doi.org/10.1038/s42003-025-07992-2
8. Das, S., Idate, R., Cronise, K. E., Gustafson, D. L. & Duval, D. L. Identifying candidate druggable targets in canine cancer cell lines using whole-exome sequencing. *Mol. Cancer Ther.* **18**, 1460–1471 (2019).
9. Beck, J. et al. Canine and murine models of osteosarcoma. *Veterinary Pathology* vol. 59 399–414 Preprint at (2022). https://doi.org/10.1177/03009858221083038
10. Mannheimer, J.D., Tawa, G., Gerhold, D. et al. Transcriptional profiling of canine osteosarcoma identifies prognostic gene expression signatures with translational value for humans. *Commun Biol* **6**, 856 (2023). https://doi.org/10.1038/s42003-023-05208-z
11. Kantarjian, H. M., O'Brien, S. & Cortes, J. Homoharringtonine/omacetaxine mepesuccinate: The long and winding road to food and drug administration approval. *Clinical Lymphoma, Myeloma and Leukemia*. **13,** 530–533 (2013). https://doi.org/10.1016/j.clml.2013.03.017
12. Winer, E. S. & DeAngelo, D. J. A review of omacetaxine: A chronic myeloid leukemia treatment resurrected. *Oncol. Ther.* **6**, 9–20 (2018).
13. Tujebajeva, R. M., Graifer, D. M., Karpova, G. G. & Ajtkhozhina, N. A. Alkaloid homoharringtonine inhibits polypeptide chain elongation on human ribosomes on the step of peptide bond formation. *FEBS Lett.* **257**, 254–256 (1989).
14. Wang, W. et al. Homoharringtonine: mechanisms, clinical applications and research progress. *Frontiers in Oncology.* **15,** (2025). https://doi.org/10.3389/fonc.2025.1522273
15. Madden, S. K., de Araujo, A. D., Gerhardt, M., Fairlie, D. P. & Mason, J. M. Taking the Myc out of cancer: toward therapeutic strategies to directly inhibit c-Myc. *Molecular Cancer*. **20** (2021). https://doi.org/10.1186/s12943-020-01291-6
16. Wang, C. et al. Alternative approaches to target Myc for cancer treatment. *Signal Transduction and Targeted Therapy*. **6,** (2021). https://doi.org/10.1038/s41392-021-00500-y
17. Walker, Z. J. et al. Exploiting protein translation dependence in multiple myeloma with omacetaxine-based therapy. *Clin. Cancer Res.* **27**, 819–830 (2021).
18. Chen, X. J. et al. Homoharringtonine deregulates MYC transcriptional expression by directly binding NF-κB repressing factor.. *Proc. Natl. Acad. Sci. U. S. A.* **116**, 2220–2225 (2019).
19. Lizardo, M. M. et al. Pharmacologic inhibition of EIF4A blocks NRF2 synthesis to prevent osteosarcoma metastasis. *Clin. Cancer Res.* **30**, 4464–4481 (2024).
20. Oblinger, J.L., Wang, J., Wetherell, G.D. et al. Anti-tumor effects of the eIF4A inhibitor didesmethylrocaglamide and its derivatives in human and canine osteosarcomas. *Sci Rep* **14**, 19349 (2024). https://doi.org/10.1038/s41598-024-69171-3
21. Thomas, L. R. & Tansey, W. P. Proteolytic Control of the Oncoprotein Transcription Factor Myc. In *Advances in Cancer Research*. **110** 77–106 (Academic Press Inc., 2011).
22. Hann, S. R. & Eisenman, R. N. Proteins encoded by the human c-myc oncogene: Differential expression in neoplastic cells. *Mol. Cell. Biol.* **4**, 2486–2497 (1984).
23. Fowles, J. S., Dailey, D. D., Gustafson, D. L., Thamm, D. H. & Duval, D. L. The Flint Animal Cancer Center (FACC) Canine Tumour Cell Line Panel: A resource for veterinary drug discovery, comparative oncology and translational medicine. *Vet. Comp. Oncol.* **15**, 481–492 (2017).
24. O'Donoghue, L. E., Rivest, J. P. & Duval, D. L. Polymerase chain reaction-based species verification and microsatellite analysis for canine cell line validation. *J. Vet. Diagn. Invest.* **23**, 780–785 (2011).
25. Farrell, K. B., Das, S., Nordeen, S. K., Lambert, J. R. & Thamm, D. H. VDX-111 targets proliferative pathways in canine cancer cell lines. *PLoS One* **19**(5): e0303470. https://doi.org/10.1371/journal.pone.0303470
26. Dobin, A. et al. STAR: Ultrafast universal RNA-seq aligner. *Bioinformatics* **29**, 15–21 (2013).
27. Liao, Y., Smyth, G. K. & Shi, W. FeatureCounts: An efficient general purpose program for assigning sequence reads to genomic features. *Bioinformatics* **30**, 923–930 (2014).
28. Love, M.I., Huber, W. & Anders, S. Moderated estimation of fold change and dispersion for RNA-seq data with DESeq2. *Genome Biol* **15**, 550 (2014). https://doi.org/10.1186/s13059-014-0550-8
29. Wu, T. et al. clusterProfiler 4.0: A universal enrichment tool for interpreting omics data. *Innovation* **2**:3, https://doi.org/10.1016/j.xinn.2021.100141.(2021).
30. Subramanian, A. et al. Gene set enrichment analysis: A knowledge-based approach for interpreting genome-wide expression profiles. *Proc. Natl. Acad. Sci. U. S. A.* **102**, 15545–15550 (2005).
31. Garcia-Alonso, L. et al. Transcription factor activities enhance markers of drug sensitivity in cancer. *Cancer Res.* **78**, 769–780 (2018).
32. Farrell, K. B., Zinnen, S., Thamm, D. H. & Karpeisky, A. Gemcitabine-Ibandronate Conjugate Enables the Bone-Targeted Combination Therapy in Bone Cancer: Synthesis and efficacy in combination with docetaxel. *Bioconjug. Chem.* **32**, 2530–2539 (2021).
33. Ianevski, A., Giri, A. K. & Aittokallio, T. SynergyFinder 3.0: An interactive analysis and consensus interpretation of multi-drug synergies across multiple samples. *Nucleic Acids Res.* **50**, W739–W743 (2022).
34. Nemunaitis, J. et al. Pharmacokinetic study of omacetaxine mepesuccinate administered subcutaneously to patients with advanced solid and hematologic tumors. *Cancer Chemother. Pharmacol.* **71**, 35–41 (2013).
35. Megquier K, Turner-Maier J, Morrill K, Li X, Johnson J, et al. (2022) The genomic landscape of canine osteosarcoma cell lines reveals conserved structural complexity and pathway alterations. *PLOS ONE* **17**(9): e0274383. https://doi.org/10.1371/journal.pone.0274383
36. Broad DepMap Portal. *DepMap Public 25Q2* depmap.org (2025).
37. Arafeh, R., Shibue, T., Dempster, J. M., Hahn, W. C. & Vazquez, F. The present and future of the Cancer Dependency Map. *Nat. Rev. Cancer*. **25**, 59–73 (2025).
38. Marhin, W. W., Chen, S., Facchini, L. M., Fornace, A. J. & Penn, L. Z. Myc represses the growth arrest gene gadd45. *Oncogene* **14**, 2825–2834 (1997).
39. Mohamed-Hadley, A., Gibbs, J. D., Liebermann, D. A. & Hoffman, B. Gadd45a behaves as a tumor suppressor and Gadd45b behaves as an oncogene in myc-mediated block in myeloid differentiation. *Blood* **110**, 4163–4163 (2007).

40. Pakjoo, M., Ahmadi, S.E., Zahedi, M. et al. Interplay between proteasome inhibitors and NF-κB pathway in leukemia and lymphoma: a comprehensive review on challenges ahead of proteasome inhibitors. *Cell Commun Signal* **22**, 105 (2024). https://doi.org/10.1186/s12964-023-01433-5
41. Sung, M. H. et al. Dynamic effect of bortezomib on nuclear factor-κB activity and gene expression in tumor cells. *Mol. Pharmacol.* **74**, 1215–1222 (2008).
42. Sogbein, O. et al. Bortezomib in cancer therapy: Mechanisms, side effects, and future proteasome inhibitors. *Life Sci.* **358** (2024). https://doi.org/10.1016/j.lfs.2024.123125
43. Meuten, T. K., Dean, G. A., Thamm, D. H. & Review The PI3K-AKT-mTOR signal transduction pathway in canine cancer. *Vet. Pathol.* **61,** 339–356 (2024). https://doi.org/10.1177/03009858231207021
44. Pyuen AA, Meuten T, Rose BJ, Thamm DH. In vitro effects of PI3K/mTOR inhibition in canine hemangiosarcoma. *PLOS ONE* **13**(7): e0200634. (2018) https://doi.org/10.1371/journal.pone.0200634
45. Li, L. et al. Protein synthesis inhibitor omacetaxine is effective against hepatocellular carcinoma. *JCI Insight* **6**, (2021). https://doi.org/10.1172/jci.insight.138197
46. Walker, Z. J. et al. Ribosome profiling reveals translational reprogramming via mTOR activation in omacetaxine-resistant multiple myeloma. *Mol. Cancer Res.* **23**, 611–621 (2025).
47. Zhang J, Chen B, Wu T, Wang Q, Zhuang L, et al. (2015) Synergistic Effect and Molecular Mechanism of Homoharringtonine and Bortezomib on SKM-1 Cell Apoptosis. *PLOS ONE* **10**(11): e0142422. (2015) https://doi.org/10.1371/journal.pone.0142422
48. Nguyen, T., Parker, R., Zhang, Y. et al. Homoharringtonine interacts synergistically with bortezomib in NHL cells through MCL-1 and NOXA-dependent mechanisms. *BMC Cancer* **18**, 1129 (2018). https://doi.org/10.1186/s12885-018-5018-x
49. Micalizzi, D. S., Ebright, R. Y., Haber, D. A. & Maheswaran, S. Translational regulation of cancer metastasis. *Cancer Res.* **81**, 517–524 (2021).
50. Lee, L. J. et al. Cancer Plasticity: The Role of mRNA Translation. *Trends in Cancer.* **7,** 134–145 (2021). https://doi.org/10.1016/j.trecan.2020.09.005
51. Ebright, R. Y. et al. Deregulation of ribosomal protein expression and translation promotes breast cancer metastasis. *Science* **367**, 1468 (2020).
52. Yu, W. et al. Homoharringtonine in combination with cytarabine and aclarubicin in the treatment of refractory/relapsed acute myeloid leukemia: A single-center experience. *Ann. Hematol.* **92**, 1091–1100 (2013).

Acknowledgements

We thank Becca Makii for mouse tissue work, and Rupa Idate and Dawn Duval for steady-state RNAseq data and maintenance of the canine cancer cell lines at the Flint Animal Cancer Center.

Author contributions

KBF performed in vitro and in vivo assays, statistical analysis, figure design, and wrote the main manuscript draft. SD designed and performed bioinformatics analysis and created figures representing sequencing data. DHT conceptualized the study, contributed experimental design, and obtained funding. All authors revised and approved final manuscript.

Funding

Partial funding for this project was provided by Cancer League of Colorado and the University of Colorado Comprehensive Cancer Center support grant P30CA046934.

Declarations

Competing interests

The authors declare no competing interests.

Additional information

Supplementary Information The online version contains supplementary material available at https://doi.org/10.1038/s41598-026-49566-0.

Correspondence and requests for materials should be addressed to K.B.F.